Journal of Photoscience (2000), Vol. 7(3), pp. 97 - 101

Electronic Spectroscopy and Ligand Field Analysis of *mer*-Chloro(1,2-ethanediamine)(1,5,9-triazanonane)chromium(III) Tetrachlorozincate(II)

Jong-Ha Choi[1]* and Yu Chul Park[2] and Hag-Sung Kim[3]
[1]Department of Applied Chemistry, Andong National University, Andong 760-749, Korea
[2]Department of Chemistry, Kyungpook National University, Daegu 702-701, Korea
[3]Department of Industrial Chemistry, Ulsan College, Ulsan 680-749, Korea

The 77 K emission and excitation spectra, and 298 K infrared and absorption spectra of *mer*-[CrCl(en)(dpt)]$ZnCl_4$ (en=1,2-diaminoethane; dpt=1,5,9-triazanonane) have been measured. Ligand field electronic transitions due to spin-allowed and spin-forbidden are assigned. The zero-phonon line in the excitation spectrum splits into two components by 151 cm^{-1}, and the large ^2E_g splitting can be reproduced by the modern ligand field theory. It is confirmed that nitrogen atoms of the en and dpt ligands have a strong σ-donor character, but chloride ligand has weak σ- and π-donor properties toward chromium(III) ion.

key words: Electronic transitions; AOM parameters; Chromium(III)

INTRODUCTION

The chromium(III) doped crystals are promising materials for tunable solid state laser in the spectral region between 600 and 1100 nm [1]. As a prerequisite for these applications, a detailed study of the spectroscopic and ligand field properties is needed. The synthesis, kinetics, absorption spectral data and structural characterization of the *mer*-chloro(1,2-ethanediamine)(1,5,9-triazanonane) chromium(III) system have been studied [2-4]. However, the vibrational and electronic energy levels based on the emission and excitation spectroscopy of this complex have not been published yet. It has been recognized that the intraconfiguration *d-d* transitions may be useful to determine metal-ligand bonding property as well as molecular geometry [5-10]. Especially, the sharp-line splittings are very sensitive to the exact bond angles around the metal. Thus it is possible to extract geometric information from the electronic spectroscopy, especially in noncrystalline environments [11,12].

In this study, the emission, excitation and infrared spectra of *mer*-[CrCl(en)(dpt)]$ZnCl_4$ (en=1,2-diaminoethane; dpt=1,5,9-triazanonane) were measured. The vibrational intervals of the electronic ground state were determined by measuring the infrared and emission spectra. The pure electronic origins due to spin-allowed and spin-forbidden transitions were assigned by analyzing the absorption and excitation spectra. Using observed electronic transitions, a ligand field analysis has been performed to determine the detailed bonding properties for the coordinated chloride and nitrogen atoms toward chromium(III) ion.

*To whom correspondence should be addressed.
E-mail : jhchoi@andong.ac.kr
Received 1 August 2000; accepted 30 August 2000

MATERIALS AND METHODS

The synthetic method of *mer*-[CrCl(en)(dpt)]$ZnCl_4$ has been reported [2]. The microcrystalline samples were generously supplied by Professor Donald A. House. The compound was recrystallized three times for spectroscopic measurements.

The 77 K emission and excitation spectra of microcrystalline sample were measured on a Spex Fluorolog-2 FL212 spectrofluorometer under the conditions previously described in details [13]. The mid-infrared spectrum was obtained with a Mattson Infinities series FT-IR spectrometer using a KBr pellet. The room temperature visible absorption spectrum was recorded with a Hewlett-Packard 8452A diode array spectrophotometer.

RESULTS AND DISCUSSION

Vibrational Intervals

The infrared spectrum of *mer*-[CrCl(en)(dpt)]$ZnCl_4$ recorded at room temperature are presented in Fig. 1.

The N-H wagging mode appears at 1280 cm^{-1} as a medium band. The N-H stretching mode near 2850 cm^{-1} for the secondary amine in dien is characteristic of meridional isomers [14]. For the dpt, we can also expect the secondary amine N-H stretching mode near 2850 cm^{-1}. There is a corresponding medium intense peak at 2880 cm^{-1} in mer-[Cr(dpt)Cl_3] [15]. This confirms that this band can be used to distinguish meridional from facial isomers. The medium

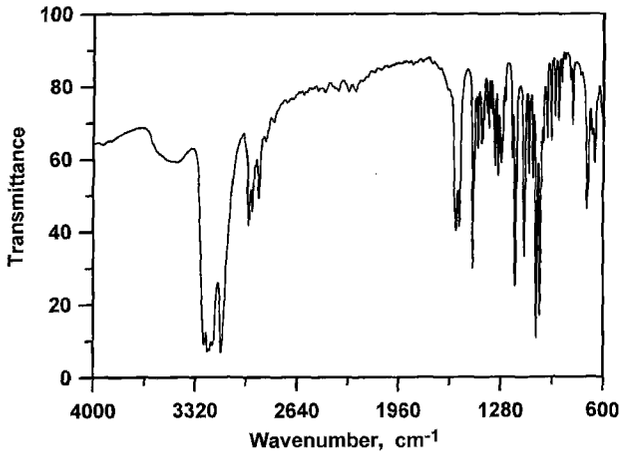

Figure 1. Infrared spectrum of *mer*-[CrCl(en)(dpt)]$ZnCl_4$ at 298 K.

intensity band at 2896 cm^{-1} shows that this band is characteristic of meridional coordination. This confirms that this band can be used to distinguish meridional from facial isomers. The strong peaks at 455 and 478 cm^{-1} can be assigned to the Cr-N stretching mode.16 A number of absorption bands below 397 cm^{-1} arise from lattice vibration, skeletal bending and the Cr-Cl stretching mode. The vibrational intervals of the electronic ground state can be obtained by comparing the emission spectrum with infrared spectral data.

The 526 nm excited 77 K emission spectrum of *mer*-[CrCl(en)(dpt)]$ZnCl_4$ is shown in Fig. 2. The band positions relative to the lowest zero phonon line, R_1, with corresponding infrared frequencies, are listed in Table 1. The vibrational fine structure of the ground state is observed. The emission spectrum except the overall intensities did not vary with exciting wavelength within the first spin-allowed transition region.

The strongest peak at 14507 cm^{-1} is assigned as the zero-phonon line, R_1, because a corresponding strong peak is found at 14510 cm-1 in the excitation spectrum. A well defined

Table 1. Vibrational frequencies from the 77 K emission and 298 K infrared spectra for *mer*-[CrCl(en)(dpt)]$ZnCl_4$[a].

Emission[b]	Infrared	Assignment
-147 m		R_2
0 vs		R_1
121 m		
215 m	225 w	Lattice vib., ring def., and ν(Cr-Cl)
278 w	280 s	
343 w	335 m	
373 s	380 m, 397 w	
444 m	428 m, 455 m	ν(Cr-N)
	478 w	
517 w	510 m, 542 s	ν(Cr-N)+Ring def.
680 w	660 m, 670 w	
708 vw	705 s	
	808 m, 820 w	$\rho(NH_2)$
840 vw	858 vw, 878 w	
901 vw	899 s, 922 m	$\rho(NH_2)$
962 vw	942 vs, 979 m	

[a] Data in cm^{-1}. [b] Measured from zero-phonon line at 14507 cm^{-1}.

hot band at 14654 cm^{-1} may be assigned to the second component of the $^2E_g \rightarrow {}^4A_{2g}$ transition. The vibronic intervals occurring in the spectrum consist of several modes that can be presumed to involve primarily lattice vibration, ring torsion and Cr-Cl stretching mode in the range 121-373 cm^{-1}. The Cr-N stretching mode was observed at 444 cm^{-1}.

Spin-forbidden Transitions

The 77 K excitation spectrum is shown in Fig. 3. The spectrum was obtained by monitoring the emission intensity of the no phonon or the vibronic sidebands at 707 nm. The shape and peak maxima of the spectrum was independent of the vibronic peak used to monitor it. The peak positions and their assignments are tabulated in Table 2. The calculated frequencies in parentheses were obtained by using the frequency

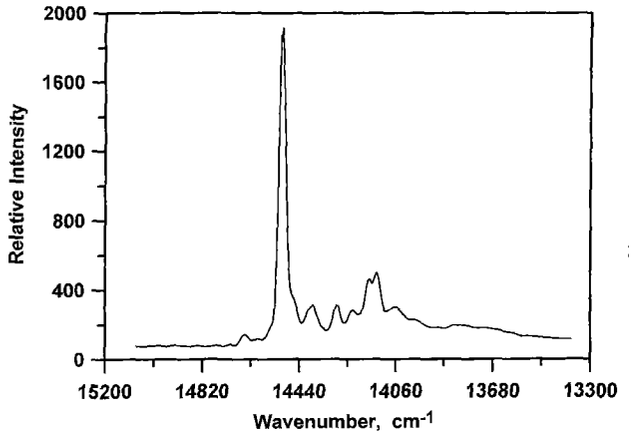

Figure 2. The 77 K emission spectrum of microcrystal *mer*-[CrCl(en)(dpt)]$ZnCl_4$ (λ_{ex} = 526 nm).

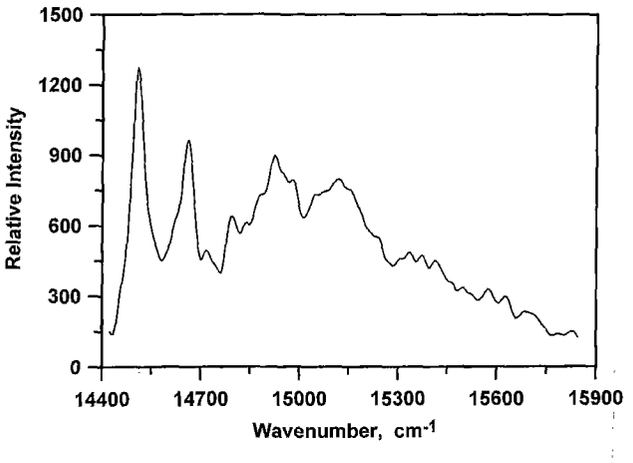

Figure 3. The 77 K excitation spectrum of microcrystal *mer*-[CrCl(en)(dpt)]$ZnCl_4$ (λ_{em} = 707 nm).

Table 2. Assignment of sharp-line positions in the 77 K excitation spectrum of *mer*-[CrCl(en)(dpt)]$ZnCl_4$[a].

$\bar{\nu}_0$-14510	Assignment	(Calcd)[b]		Vibronic frequencies[c]	Ground state frequencies[d]
0 vs	R_1		ν_1	47	?
48 sh	$R_1 + \nu_1$	(47)	ν_2	123	121
112 sh	$R_1 + \nu_2$	(123)	ν_3	212	215
151 vs	R_2		ν_4	289	280
207 m	$R_1 + \nu_3$	(212)	ν_5	384	380
285 m	$R_1 + \nu_4$	(289)	ν_6	448	444
327 w	$R_2 + \nu_1 + \nu_2$	(321)			
371 sh	$R_2 + \nu_3$	(363)			
413 vs	T_1				
440 sh	$R_2 + \nu_4$	(440)			
469 m	T_2				
539 w	$T_1 + \nu_2$	(536)			
568 w	$R_2 + \nu_2 + \nu_4$	(563)			
609 s	T_3				
651 sh	$R_2 + \nu_1 + \nu_6$	(646)			
674 sh	$T_1 + \nu_1 + \nu_3$	(672)			
729 w	$T_2 + \nu_1 + \nu_3$	(728)			
799 w	$T_1 + \nu_5$	(797)			
825 m	$T_1 + \nu_2 + \nu_4$	(825)			
863 m	$T_1 + \nu_6$	(861)			
903 m	$T_3 + \nu_4$	(898)			
958 w					
989 w	$T_3 + \nu_5$	(993)			
1020 sh	$T_3 + \nu 2 + \nu_4$	(1021)			
1066 m	$T_2 + \nu_3 + \nu_5$	(1065)			
1120 m	$T_3 + \nu_2 + \nu_5$	(1116)			
1174 w	$T_1 + 2\nu_5$	(1181)			
1208 vw	$T_2 + \nu_4 + \nu_6$	(1206)			
1243 sh	$T_1 + \nu_5 + \nu_6$	(1245)			
1273 vw	$T_3 + \nu_3 + \nu_6$	(1269)			

[a] Data in cm^{-1}. [b] Values in parentheses represent the calculated frequencies based on the vibrational modes listed. [c]From the excitation spectrum. [d]From the emission and infared spectra.

values of vibrational modes $\nu_1 \sim \nu_6$ listed in Table 2.

Two strong peaks at 14510 and 14661 cm^{-1} in the excitation spectrum are assigned to the two components (R_1 and R_2) of the $^4A_{2g} \rightarrow {}^2E_g$ transition. The lowest-energy zero-phonon line coincides with the emission origin within 3 cm^{-1}. The zero-phonon line in the excitation spectrum splits into two components by 151 cm^{-1}, and it is comparable to values for other tetragonal chromium(III) complexes [8-10]. In general, it is not easy to locate positions of the other electronic components because the vibronic sidebands of the ^2E_g levels overlap with the zero phonon lines of $^2T_{1g}$. However, the three components of the $^4A_{2g} \rightarrow {}^2T_{1g}$ electronic origin (T_1, T_2 and T_3) are assigned to relative intense peaks at 413, 469 and 609 cm-1 from the lowest electronic line, R1 because they have no correspondence in emission. Vibronic satellites based on these origins also have similar frequencies and intensity patterns to those of the ^2E_g components.

The higher energy $^4A_{2g} \rightarrow {}^2T_{2g}$ band was found at 20942 cm^{-1} from the second derivative of the solution absorption spectrum, as shown with dotted line in Figure 4. It could not

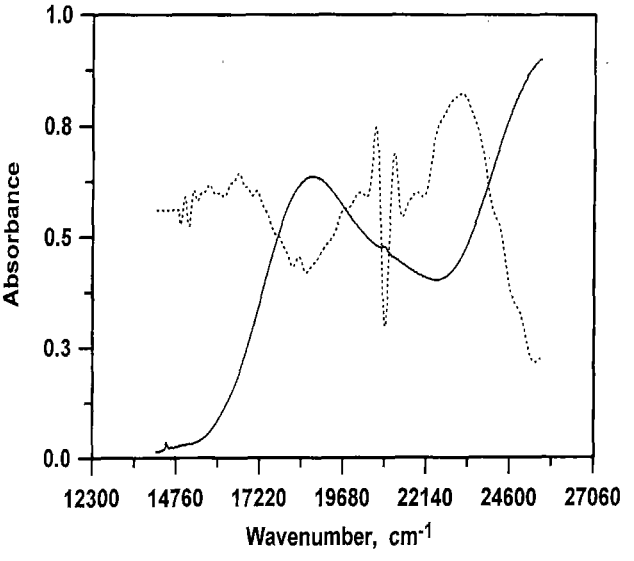

Figure 4. Absorption spectrum (solid line) and second derivative (dotted line) of *mer*-$[CrCl(en)(dpt)]^{2+}$ in aqueous solution.

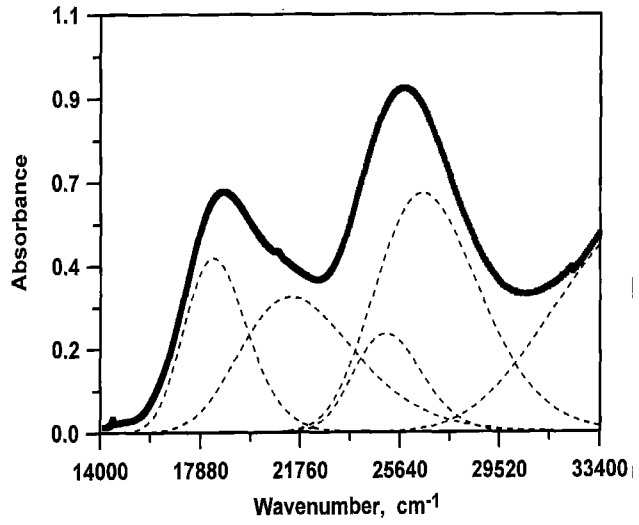

Figure 5.Electronic absorption spectrum of *mer*-[CrCl(en)(dpt)]$^{2+}$ in aqueous solution at 298 K.

be resolved into the separate components.

Spin-allowed Transitions

The visible absorption spectrum (solid line) of *mer*-[CrCl(en)(dpt)]$^{2+}$ in aqueous solution at room temperature is represented in Fig. 5.

It exhibits two bands, one at 18727 cm^{-1} (ν_1) and the other at 25806 cm^{-1} (ν_2), corresponding to the $^4A_{2g} \rightarrow {}^4T_{2g}$ and $^4A_{2g} \rightarrow {}^4T_{1g}$ (O_h) transitions, respectively [16]. The dotted lines represent the result of Gaussian analysis. The second quartet band has nearly symmetric profiles. However, in order to obtain some points of reference for the splittings of the two bands, the band profiles were fitted by using four Gaussian curves. A deconvolution procedure on the experimental band pattern yielded four maxima at 18522, 19107, 25501 and 25930 cm^{-1} for the noncubic splittings of $^4T_{2g}$ and $^4T_{1g}$. These resolved peak positions were adapted for the spin-allowed transition energies in the ligand field optimization.

Ligand Field Analysis

Ligand field calculation were carried out in the framework of the angular overlap model using the AOMX program [18] described in several previous our publications [7-11,19]. The ligand field potential matrix was assumed to arise only from the one chloride and five nitrogen atoms. The angular positions of coordinated chloride and nitrogens were taken from the X-ray crystal structure [2] of mer-[CrCl(en)(dpt)]$ZnCl_4$, which was determined to be monoclinic with the space group P21. The coordinates were then rotated so as to maximize the projections of the six-coordinated nitrogen atoms on the Cartesian axes centered on the chromium. The resulting Cartesian and spherical coordinates are shown in Table 3.

The model parameters are e_σ(Cl) and e_π(Cl) for the chloride-chromium, $e_\sigma(N_{pri})$ and $e_\sigma(N_{sec})$ for the en and dpt nitrogen-chromium, Racah parameters B and C for the inter-electronic repulsion, parameter T for the Trees correction and parameter ζ for the spin-orbit coupling. The π-interaction of amine nitrogens with sp^3 hybridization in the en and dpt was assumed to be negligible. However, it is noteworthy that the peptide nitrogen with sp^2 hybridization has a weak π-donor character [20]. All parameters, except e_σ(Cl) and e_π(Cl), were constrained to reasonable limits based on the data from other chromium(III) complexes. The nine parameters were used to fit eleven experimental energies: the five $^4A_{2g} \rightarrow \{^2E_g, {}^2T_{1g}\}$ components, identified in Table 4, the average energy of the transition to the $^2T_{2g}$ state, the four $^4A_{2g} \rightarrow \{^4T_{2g}, {}^4T_{1g}\}$ components, and the splitting of the ^2E_g state. Eigenvalues were assigned to states within the doublet and quartet manifolds based on an analysis of the corresponding eigenfunctions. Fitting of parameters to the electronic spectra was performed using the Powell parallel subspace optimization procedure [21]. The optimization was repeated

Table 3. Optimized Cartesian and spherical polar coordinates for ligating nitrogen atoms in *mer*-[CrCl(en)(dpt)]$ZnCl_4$[a].

Atom	x	y	z	θ	ϕ
Cl(1)	-0.0067	-2.3257	0.0081	89.80	-90.17
N(1)	-0.0120	0.0188	-2.3326	179.45	122.55
N(2)	2.0261	-0.0641	-0.1567	94.42	-1.81
N(3)	0.0639	-2.0307	0.1736	85.12	-88.20
N(4)	-2.0261	0.0641	0.1567	85.58	178.19
N(5)	-0.0639	2.0307	-0.1736	94.88	91.80

[a]Cartesian coordinates in Å, polar coordinates in degrees.

Table 4. Experimental and calculated electronic transition energies for *mer*-[CrCl(en)(dpt)]$ZnCl_4$[a].

State (O_h)	Exptl	Calcd[b]
^2E_g	14510	14421
	14661	14569
$^2T_{1g}$	14923	14962
	14979	15047
	15119	15071
$^2T_{2g}(avg.)$	20942	22068
$^4T_{2g}$	18365[c]	19117
	21390[c]	21328
$^4T_{1g}$	25094[c]	24732
	26596[c]	27200

[a]Data in cm^{-1}. [b]$e_\sigma(N_{pri})$ = 7125±35, $e_\sigma(N_{sec})$ = 7542±30, e_σ(Cl) = 5824±45, e_π(Cl) = 882±15, B = 700±4, C = 3182±16, α_T = 36±2, ζ = 165±18, τ= 0.993. [c]Obtained from the Gaussian component deconvolution.

several times with different sets of starting parameters to verify that the same global minimum was found. The results of the optimization and the parameter set used to generate the best-fit energies are also listed in Table 4. This procedure proved to show good fit for the sharp line transitions. The error margins reported for the best-fit parameters in Table 4 are based only on the propagation of the assumed uncertainties in the observed peak positions [22]. The quartet terms were given a very low weight to reflect the very large uncertainty in their position.

The following values were finally obtained for the ligand field parameters: $e_\sigma(N_{pri})$ = 7125±35, $e_\sigma(N_{sec})$ = 7542±30, e (Cl) = 5824±45, e_σ(Cl) = 882±15, B = 700±4, C = 3182 ±16, α_T = 36±2, ζ= 165±18 cm^{-1}. The π-orbital expansion parameter τ was found at the value 0.993. A ligand field analysis of the sharp-line excitation and broad-band absorption spectra indicates that the chloride is a weak σ-and π-donor. The values of 7125 and 7542 cm^{-1} for primary and secondary amine nitrogens are comparable to values for other amines [23-26]. It is confirmed that the nitrogen atoms of the en and dpt ligands have strong σ-donor properties toward chromium(III) ion. The secondary amine group of 1,5,9-triazanonane has a larger value than that of the primary amine group. An orbital population analysis of yields a configuration of $(xy)^{1.003}(z)^{0.975}(yz)^{0.979}(x^2\text{-}y^2)^{0.018}(z^2)^{0.095}$ for the lowest component of the ^2E_g state. The relative d-orbital ordering from the calculation is $E(xy)$ = 122 cm^{-1} < $E(xz)$ = 908 cm^{-1} < $E(yz)$ = 1194 cm^{-1} < $E(x^2\text{-}y^2)$ = 19946 cm^{-1} < $E(z^2)$ = 21460 cm^{-1}. These factors plus AOM parameters can be used in predicting the photolabilized ligand and the relative quantum yields of the photoinduced reaction [27]. The value of the Racah parameter, B is about 76 % of the value for a free chromium(III) ion in the gas phase. The 151 cm^{-1} of observed ^2E_g splitting in the excitation spectrum is slightly smaller than the 198 cm^{-1} of *cis*-[Cr(trien)Cl$_2$]Cl [8]. It is shown that the large ^2E_g splitting can be reproduced by the modern ligand field theory. The parameter values reported here appear to be significant, as deduced on the basis of the manifold of sharp-line transitions which were obtained from the highly resolved excitation spectrum. The information on electronic and vibrational levels of this complex may be useful to create a good spectroscopic basis of knowledge for the further development of new laser materials.

Acknowledgement – This work was financially supported by Korea Research Foundation Grant(KRF-2000-DP-0217) and partially Brain Korea 21 project. We wish to thank Professor Donald A. House for a gift of the title compound. One of us (Choi, J. H) also wish to thank Prof. H. U. G del, University of Bern, Switzerland for giving the opportunity to visit his laboratory and use his equipment.

REFERENCES

1. Powell, R. C (1998) Physics *of Solid-State Laser Materials*, Springer- Verlag, New York.
2. House, D. A. and W. T. Robinson (1988) Chromium(III) complexes with 1,5,9-triazanonane (3,3-tri)-CrX$_3$(3,3-tri)$^{n+}$ and CrCl(diamine)(3,3,-tri)$^{2+}$. *Inorg. Chim. Acta* **141**, 211-220.
3. House, D. A., Reddy, K. Bal. and R. van Eldik (1991) Activation volumes for the base hydrolysis of some chloro (diamine)(triamine)chromium(III) complexes. *Inorg. Chim. Acta* **186**, 5-10.
4. House, D. A. and R. van Eldik (1995) Pressure effects on the rates of Hg^{2+}-assisted chloride release from some [CrCl(diamine)(triamine)]$^{2+}$ complexes. *Inorg. Chim. Acta* **230**, 29-34.
5. Hoggard, P. E (1994) Sharp line electronic spectra and metal ligand geometry. *Top. Curr. Chem.* **171**, 114-141.
6. Sch nherr, T (1997) Angular overlap model applied to transition metal complexes and d^N-ions in oxide host lattices. *Top. Curr. Chem.* **191**, 87-152.
7. Choi, J. H. and I. G. Oh (1997) Sharp-line electronic spectroscopy and ligand field analysis of [Cr(*trans*-diammac)](ClO$_4$)$_3$. *Bull. Korean Chem. Soc.* **18,** 23-27.
8. Choi, J. H (1998) Emission, excitation and far-infrared spectroscopy of *cis*-α-dichlorotriethyleneteraminechromium(III) Chloride. *Bull. Korean Chem. Soc.* **19**, 575-579.
9. Choi, J. H (1999) Spectroscopic properties and ligand field analysis of pentaammine(imidazole)chromium(III) perchlorate. *Bull. Korean Chem. Soc.* **20**, 81-84.
10. Choi, J. H (1999) High resolution optical spectroscopy of *mer*-[Cr(dpt) (Gly-Gly)]ClO$_4$. *Bull. Korean Chem. Soc.* **20**, 436-440.
11. Choi, J. H (1994) Spectroscopic properties and lignad field analysis of tris(*trans*-1,2-cyclohexanediamine)chromium(III) chloride. *Bull. Korean Chem. Soc.* **15**, 145-150.
12. Hoggard, P. E (1986) Sharp line electronic transitions and metal-ligand angular geometry. *Coord. Chem. Rev.* **70**, 85-120.
13. Choi, J. H (2000) Spectral properties and ligand field analysis of *cis*-dinitrito(1,4,8,11-tetraazacyclotetradecane)chromium(III) nitrate. *Chem. Phys.* **256**, 29-35.
14. Subramaniam, V. and P. E. Hoggard (1989) Meridional coordination ofdiethylenetriamine to chromium(III). *Inorg. Chim. Acta* **155**, 161-163.
15. Subramaniam, V. (1989) Ph.D. Thesis, North Dakota State University.
16. Nakamoto, K (1997) *Infrared and Raman Spectra of Inorganic and Coordination Compounds, Part B*, 5th Ed., John Wiley & Sons, New York.
17. Lever, A. B. P (1984) *Inorganic Electronic Spectroscopy*, Elsevier, Amsterdam.
18. Adamsky, H (1996) AOMX, A fortran computer program

for ligand field pameterization, Univ. of Düsseldorf.
19. Choi, J. H (2000) Spectroscopic properties and ligand field analysis of *cis*-diazido(1,4,8,11-tetraazacyclotetradecane) chromium(III) azide. *Spectrochim. Acta* **56A**, 1653-1660.
20. Choi, J. H. and P. E. Hoggard (1992) Ligand field properties of the peptide nitrogen. *Polyhedron* **11**, 2399-2407.
21. Kuester, J. L. and J. H. Mize (1973) *Optimization Techniques with Fortran, McGraw-Hill*, New York, pp. 331-343.
22. Clifford, A. A. (1973) *Multivariate Error Analysis,* Wiley-Hasted, New York.
23. Choi, J. H. and I. G. Oh (1993) Sharp line electronic spectroscopy and lignad field analysis of *cis*-(1,4,8,11-tetraazacyclotetradecane)(ethylendiamine) chromium(III). Bull. Korean Chem. Soc. 14, 348-352.
24. Choi, J. H (1993) Spectroscopic properties of cis-(1,4,8,11-tetraaza cyclotetradecane)(1,2-propanediamine)chromium(III). *Bull. Korean Chem. Soc.* **14**, 118-122.
25. Choi, J. H (1997) Spectroscopic properties and ligand field analysis of cis-dinitrato(1,4,8,11-tetraazacyclotetradecane)chromium(III) nitrate. Bull. Korean Chem. Soc. 18, 819-823.
26. Figgis, B. N. and M. A. Hitchman (2000) Ligand field Theory and Its Applications, Wiley-VCH, New York.
27. Vanquickenborne, L. G. and A. Ceulemans (1983) Ligand field model of and the photochemistry of coordination compounds. *Coord. Chem. Rev.* **48**, 157-202.